



OIST

OKINAWA INSTITUTE OF SCIENCE AND TECHNOLOGY GRADUATE UNIVERSITY
沖縄科学技術大学院大学

An Exception to the Carothers Equation Caused by the Accelerated Chain Extension in a Pd/Ag Cocatalyzed Cross Dehydrogenative Coupling Polymerization

Author	Liwen Xing, Ji-Ren Liu, Xin Hong, Kendall N. Houk, Christine K. Luscombe
journal or publication title	Journal of the American Chemical Society
volume	144
number	5
page range	2311-2322
year	2022-01-31
Publisher	American Chemical Society
Rights	(C) 2022 The Authors. ACS AuthorChoice with CC-BY-NC-ND.
Author's flag	publisher
URL	http://id.nii.ac.jp/1394/00002320/

doi: [info:doi/10.1021/jacs.1c12599](https://doi.org/10.1021/jacs.1c12599)

An Exception to the Carothers Equation Caused by the Accelerated Chain Extension in a Pd/Ag Cocatalyzed Cross Dehydrogenative Coupling Polymerization

Liwen Xing,[¶] Ji-Ren Liu,[¶] Xin Hong,^{*} Kendall N. Houk,^{*} and Christine K. Luscombe^{*}



Cite This: *J. Am. Chem. Soc.* 2022, 144, 2311–2322



Read Online

ACCESS |



Metrics & More

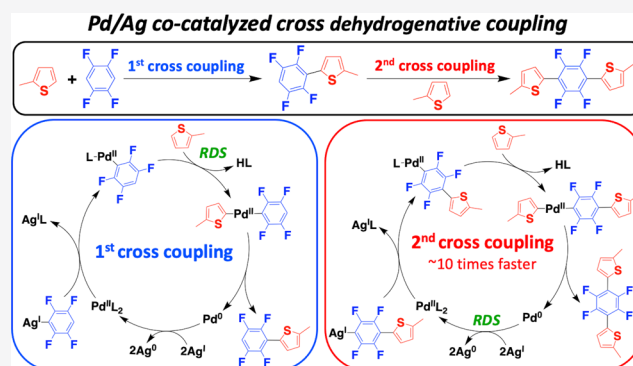


Article Recommendations



Supporting Information

ABSTRACT: The Carothers equation is often used to predict the utility of a small molecule reaction in a polymerization. In this study, we present the mechanistic study of Pd/Ag cocatalyzed cross dehydrogenative coupling (CDC) polymerization to synthesize a donor–acceptor (D–A) polymer of 3,3'-dihexyl-2,2'-bithiophene and 2,2',3,3',5,5',6,6'-octafluorobiphenyl, which go counter to the Carothers equation. It is uncovered that the second chain extension cross-coupling proceeds much more efficiently than the first cross-coupling and the homocoupling side reaction (at least 1 order of magnitude faster) leading to unexpectedly low homocoupling defects and high molecular weight polymers. Kinetic analyses show that C–H bond activation is rate-determining in the first cross-coupling but not in the second cross-coupling. Based on DFT calculations, the high cross-coupling rate in the second cross-coupling was ascribed to the strong Pd–thiophene interaction in the Pd-mediated C–H bond activation transition state, which decreases the energy barrier of the Pd-mediated C–H bond activation. These results have implications beyond polymerizations and can be used to ease the synthesis of a wide range of molecules where C–H bond activation may be the limiting factor.



INTRODUCTION

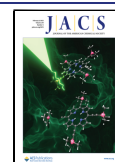
In polycondensations, the number-average degree of polymerization (DP) can be expressed as $DP = (1 + r)/(1 + r - 2rp)$, where p is the extent of the polymerization and r is the stoichiometric ratio between the comonomers. This equation was originally proposed by Carothers and is often referred to as the Carothers equation.^{1,2} The Carothers equation is based on the assumption of equal reactivity of functional groups, which means that the reactivity of one functional group of a bifunctional monomer is the same irrespective of whether the other functional group has reacted, and the reactivity of a functional group is independent of the size of the molecule to which it is attached.^{1,2} For polymerizations such as polyesterifications or polycondensation to synthesize nylon, the molecular weights of the product can be accurately predicted using the Carothers equation, since the reactivity of the functional groups in these polymerizations does not change significantly (the change of the rate constant is within 3-fold) with the size of the reactants.² In some polymerizations, however, the molecular weight of the polymer products can be significantly higher than predicted by the Carothers equation.^{3–7} For example, Endo et al. reported a polycondensation between 2,2-dichloro-1,3-benzodioxole and 4,4'-isopropylidenediphenol. A number-average molecular weight (M_n) of 120 kg/mol was obtained when 5 equiv of

dioxole and 3 equiv of diphenol were used,⁶ when an M_n of 0.693 kg/mol was predicted by the Carothers equation. This was ascribed to the rate acceleration during the polycondensation, where the rate of the first condensation reaction to form the dioxole-diphenol dimer was 27 times slower than that of the second condensation reaction between the dioxole-diphenol dimer and another diphenol. Conversely, significantly lower molecular weights than predicted by the Carothers equation can be achieved if the reactivity of the functional groups decreases as the polymerization proceeds.⁸

Donor–acceptor (D–A) conjugated polymers are attractive semiconducting polymers that have a wide range of applications in organic electronics such as organic light emitting diodes (OLEDs), organic field-effect transistors (OFETs), organic photovoltaics (OPVs), and biomedical sensors.^{9–12} The current synthetic methods for D–A conjugated polymers are usually Suzuki coupling,¹³ Stille coupling,¹⁴ and more environmentally preferable direct

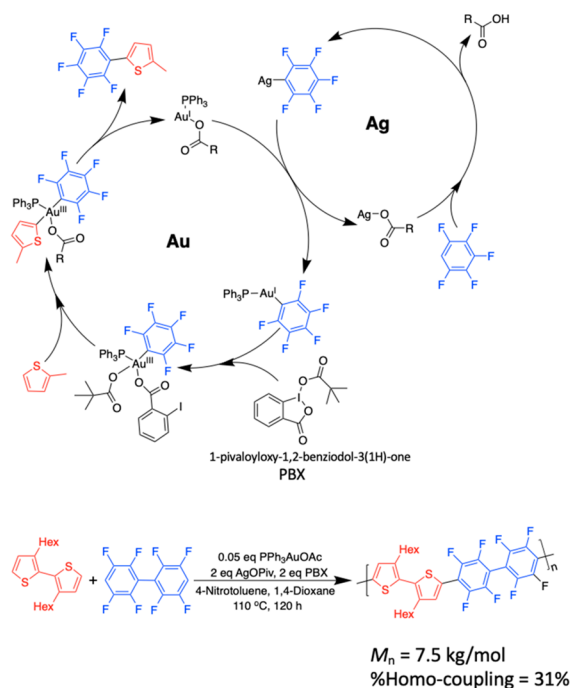
Received: November 30, 2021

Published: January 31, 2022

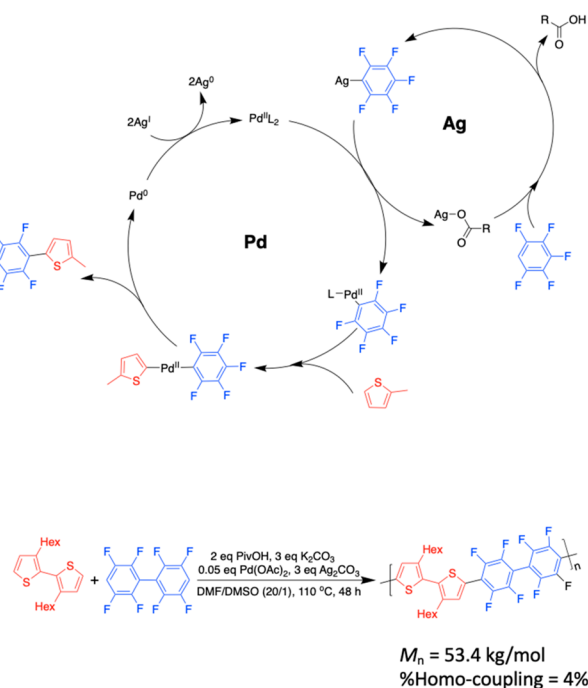


Scheme 1. (a) Proposed Mechanism for the Au/Ag Cocatalyzed CDC,^{8,24} and Results of the Polymerization;⁸ (b) Proposed Mechanism for the Pd/Ag Cocatalyzed CDC,²⁶ and Results of the Polymerization²⁰

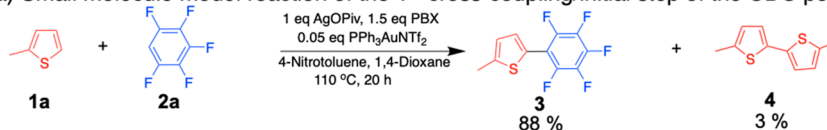
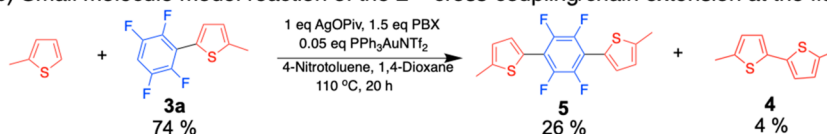
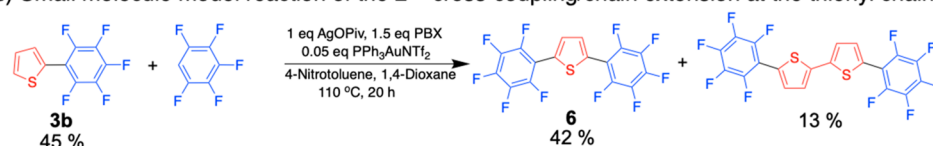
a) Au/Ag co-catalyzed CDC



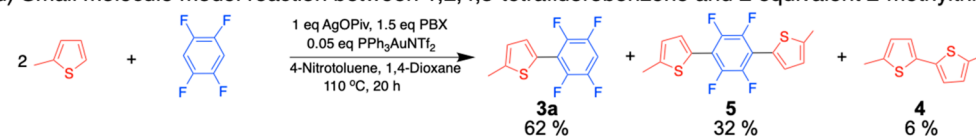
b) Pd/Ag co-catalyzed CDC



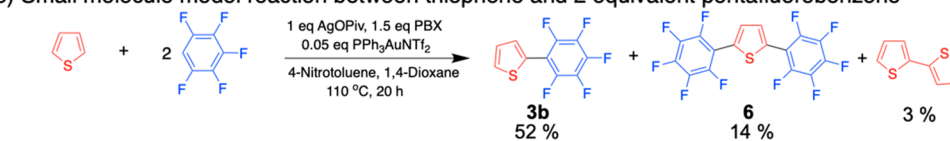
Scheme 2. Small Molecule Model Reactions for Au/Ag Cocatalyzed CDC Polymerization

a) Small molecule model reaction of the 1st cross-coupling/initial step of the CDC polymerizationb) Small molecule model reaction of the 2nd cross-coupling/chain extension at the fluorophenyl chain endc) Small molecule model reaction of the 2nd cross-coupling/chain extension at the thienyl chain end

d) Small molecule model reaction between 1,2,4,5-tetrafluorobenzene and 2 equivalent 2-methylthiophene



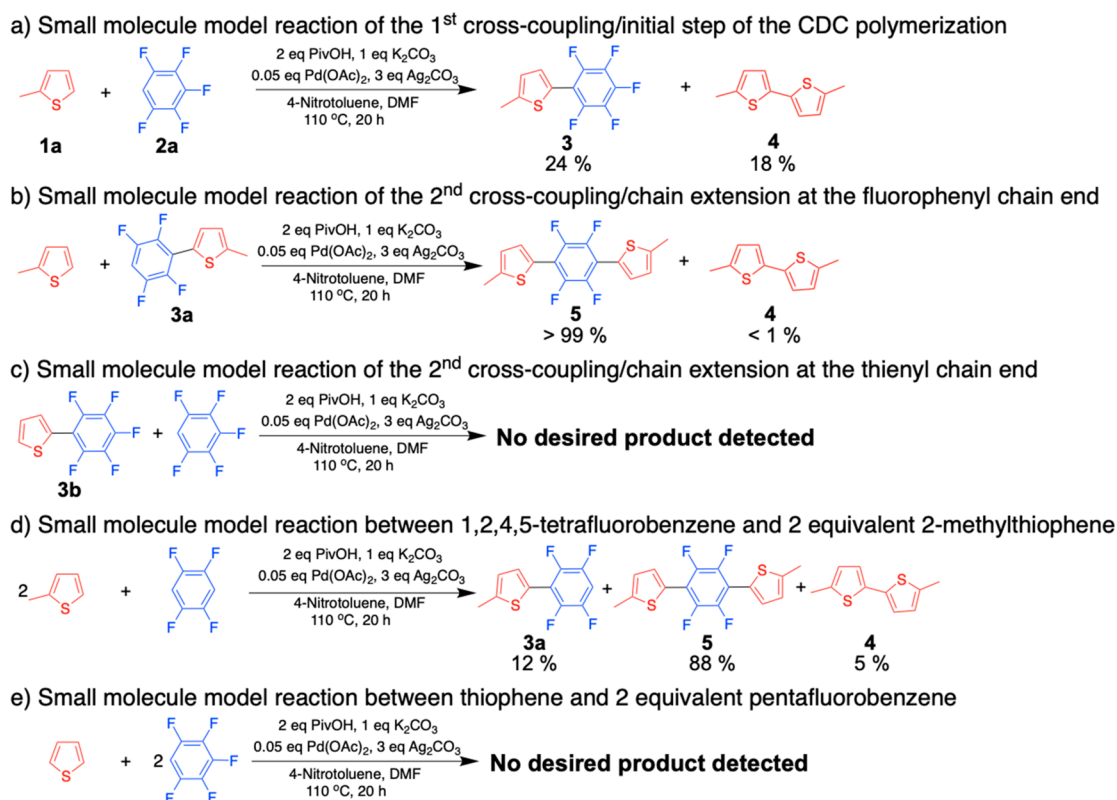
e) Small molecule model reaction between thiophene and 2 equivalent pentafluorobenzene



arylation polymerization (DARP),¹⁵ all of which require prefunctionalization of the monomers such as boronation,

stannylation, and/or halogenation. These extra prefunctionalization steps lead to generation of a large amount of hazardous

Scheme 3. Small Molecule Model Reactions for Pd/Ag Cocatalyzed CDC Polymerization



chemical waste and high costs of the polymer products, which hinders their industrial scalability and commercial viability.¹⁶ Cross dehydrogenative coupling (CDC), also known as oxidative CH/CH cross-coupling, can potentially serve as an ideal approach to D–A polymer synthesis, since it eliminates all prefunctionalization steps of monomers by directly activating C–H bonds and subsequently forming C–C bonds *in situ* during the polymerization.

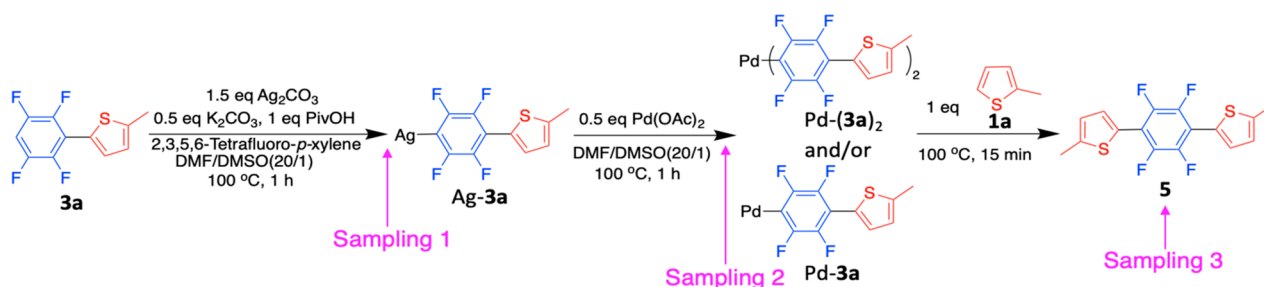
A high-performance D–A polymer usually requires a large molecular weight and perfect alternation of electron-donor and electron-acceptor repeating units along the polymer backbone.^{17,18} Unfortunately, development of an efficient CDC polymerization, also known as oxidative direct arylation polymerization (oxi-DARp), to synthesize high-performance D–A conjugated polymers remains challenging. It is difficult to achieve high chemo- and regioselectivity during the polymerizations in the presence of multiple reactive sites (C–H bonds). Specifically, the metal catalysts typically are not sufficiently selective to distinguish between the electron-rich and electron-poor monomers, which leads to homocoupling defects in the D–A polymer products.¹⁹ Thus far, limited progress has been made in this field.^{8,20–22}

Here, we present two CDC polymerizations that defy the Carothers equation. First, we briefly discuss a Au/Ag cocatalyzed CDC polymerization previously reported by our group⁸ and developed based on an efficient and highly selective small molecule CDC reported by Larossa et al.²³ Then, a Pd/Ag cocatalyzed CDC polymerization is investigated in detail.²⁰ Despite both polymerizations occurring by a similar sequence (Schemes 1a and b) where the C–H bond of the electron-poor monomer is activated by Ag and the C–H bond of the electron-rich monomer is activated by Au or Pd, we find dramatically different polymerization results. The Au/Ag

cocatalyzed CDC results in low molecular weight polymers (7.5 kg/mol) with homocoupling defects (~30%) despite the small molecule coupling reaction proceeding efficiently (Scheme 2a). The functional groups (i.e., the C–H bond) become less reactive after the first cross-coupling reaction because the tetra-fluorobenzene chain ends on the oligomer are less electron-poor than the fluorobenzene monomers, and the thiophene chain ends on the oligomer are less electron-rich than the thiophene monomers.^{8,24} Conversely, in the Pd/Ag cocatalyzed system, we find that the functional groups become more reactive after the first cross-coupling step. Specifically, in the first cross-coupling reaction, Pd-mediated C–H activation is the rate-determining step, whereas in the proceeding chain extending cross-coupling reaction, the energy barrier to break the C–H bond is reduced due to the presence of the thiophene substituent on the fluorinated benzene. While this finding has important implications in polymerizations leading to unexpectedly high molecular weight polymers and reduced homocoupling defects, these findings could affect the design of substrates in late-stage C–H functionalization.

RESULTS AND DISCUSSION

Small Molecule Model Reactions for the Au/Ag Cocatalytic System. Scheme 2 shows a series of small molecule model reactions for the Au/Ag cocatalyzed CDC polymerization. Scheme 2a represents a model reaction of the first cross-coupling of the CDC polymerization. The cross-coupling yield in this was as high as 88%, and the homocoupling yield was low (3%). The small molecule model reactions shown in Schemes 2b and 2c represent the chain extension in the CDC polymerization, in which the CDC occurs between the cross-coupled dimers (3a and 3b) and the monomers. This second cross-coupling generated the cross-

Scheme 4. Stepwise CDC Sampling Experiments to Determine the Mechanistic Sequence of the Pd/Ag Cocatalyzed Chain Extension CDC


coupled trimers **5** and **6** in low yield, and unreacted starting materials **3a** and **3b** remained. Scheme 2d and 2e show the small molecule model reactions that model the overall CDC polymerization. In these reactions, the yields of **3a** and **3b** were much higher than **5** and **6** confirming that the second cross-coupling reaction is less effective than the first.

Small Molecule Model Reactions for the Pd/Ag Cocatalytic System. Similarly, the results of the small molecule model reactions for the Pd/Ag cocatalyzed CDC polymerization are shown in Scheme 3. Scheme 3a shows the small molecule model reaction for the initial step of the CDC polymerization (the first cross-coupling). There is almost no chemoselectivity, and the product yields are low. In Scheme 3b, the chain extension step (the second cross-coupling), the trimerization of cross-coupled dimer **3a** displayed an exceptional reactivity and cross chemoselectivity (the yield of cross-coupled trimer **5** was close to 100%). In Scheme 3d the yield of the trimer **5** (88%) is much higher than that of the dimer **3a** (12%). We speculated that, in Scheme 3d, once **3a** was formed, it immediately reacted with another monomer **1a** to produce the cross-coupled trimer **5**, which drove the reaction forward. For Scheme 3c and 3e, no desired product was detected by NMR spectroscopy because both C–H bonds at the α - and β -positions of the thiophene moiety that is attached to an electron-withdrawing group (**3b**) can be activated during the reaction leading to the formation of insoluble polymeric materials.²⁵ Generally, Scheme 3 shows that the chain extension CDC proceeded more readily than the first CDC which is opposite to what was observed in the Au/Ag system in Scheme 2.

By comparing the small molecule model reactions between the Au/Ag and Pd/Ag systems, it was confirmed that the functional groups become less reactive in the Au/Ag cocatalyzed CDC polymerization, while the functional groups become more reactive in the Pd/Ag cocatalyzed CDC polymerization.

The Au/Ag cocatalyzed CDC has been studied in detail, and we can rationalize why the C–H bond of the cross-coupled dimer **3a** is less reactive than that of the monomer—the selectivity of the reaction is driven by the acidity of the proton with the acidity decreasing upon the addition of the thiophene to tetrafluorobenzene.^{8,24} We now focus on the mechanistic investigation of the Pd/Ag cocatalyzed chain extension CDC (Scheme 3b) to elucidate the factors that contribute to the high molecular weight polymer with minimal homocoupling defects using both experimental and computational methods.

Stepwise Sampling Experiments to Determine the Mechanistic Sequence of the Pd/Ag Cocatalyzed Chain Extension CDC. Our mechanistic studies for the chain extension CDC started with the stepwise CDC sampling

experiment (Scheme 4). The yield of each species was tracked using ¹⁹F NMR and is shown in Table 1.

Table 1. Yield of Each Species in the Stepwise CDC Sampling Experiment Shown in Scheme 4

Sampling	3a (%)	Ag-3a (%)	Pd-3a (%)	Pd-(3a) ₂ (%)	5 (%)
1	90	10	–	–	–
2	9	Not detected	11	60	–
3	14	Not detected	Not detected	12	64

In this sampling experiment, **3a** and Ag₂CO₃ and other additives were first mixed and heated at 100 °C for 1 h. Then, the first aliquot (sampling 1) was taken. Next, Pd(OAc)₂ was added, the reaction continued for another hour, and the second aliquot (sampling 2) was taken. Finally, **1a** was added, and after 15 min the third aliquot (sampling 3) was taken. The ¹⁹F NMR spectrum of each sampling is shown in Figure 1. In sampling 1, we observed the formation of Ag-**3a**, which indicated that the Ag-mediated C–H bond activation on **3a** occurred. After adding Pd(OAc)₂ and heating the reaction for 1 h (sampling 2), the peaks corresponding to Ag-**3a** disappeared, and the peaks corresponding to Pd complexes (Pd-**3a** and Pd-(**3a**)₂) appeared (Figure 1, middle spectrum), which suggested that transmetalation between Ag-**3a** and Pd(II) occurred in this step. Sampling 2 also showed that the bifluoroaryl Pd-(**3a**)₂ was more prevalent than the monofluoroaryl Pd-**3a**. In sampling 3, the cross-coupled trimer product **5** was detected, which implied a C–C bond formation between **3a** and **1a**. Based on the results above, we conjectured that the mechanistic sequence of the Pd/Ag cocatalyzed chain extension CDC is (1) Ag-mediated C–H bond activation on electron-poor **3a** to form Ag-**3a**; (2) Transmetalation between Ag-**3a** and Pd(II) to form Pd-**3a** and Pd-(**3a**)₂; (3) Pd-mediated C–H bond activation of the electron-rich **1a**; (4) Reductive elimination to form the cross-coupled product **5**; and then (5) Oxidation of Pd(0) by Ag(I) to reactivate the Pd catalyst. This is consistent with the mechanistic sequence of the first cross-coupling reaction uncovered by the Kanbara group (Scheme 1b).²⁶

To confirm this proposed mechanistic sequence of the chain extension step, controlled stepwise CDC sampling experiments were conducted (Scheme 5). The yield of each species is summarized in Tables S3, S4, and S5, and the NMR spectrum of each sampling is shown in Figures S1, S2, and S3 in Supporting Information. When the sequence of adding **1a** and **2a** was reversed (Scheme 5a), no cross-coupled product **3** was observed in sampling 3 according to ¹H NMR, which means the mechanistic sequence shown in Scheme 5a can be ruled

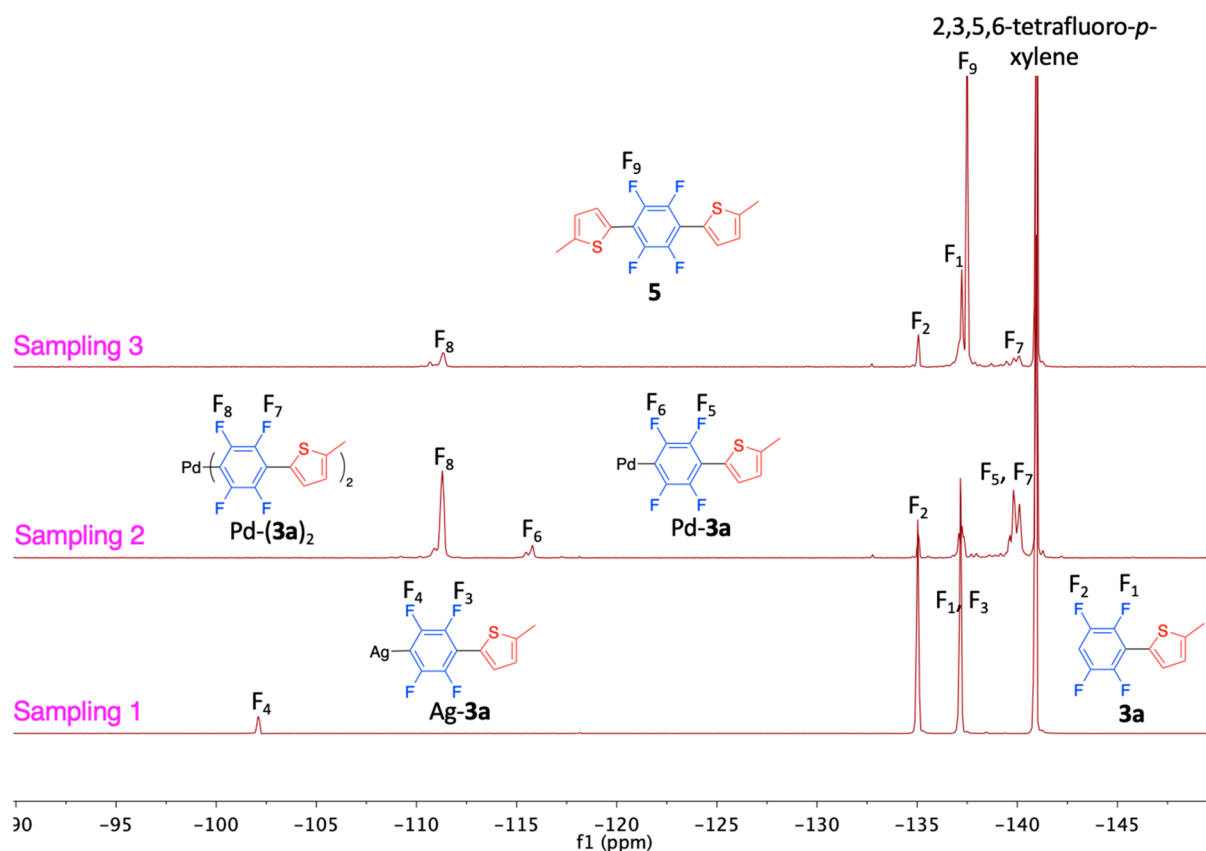


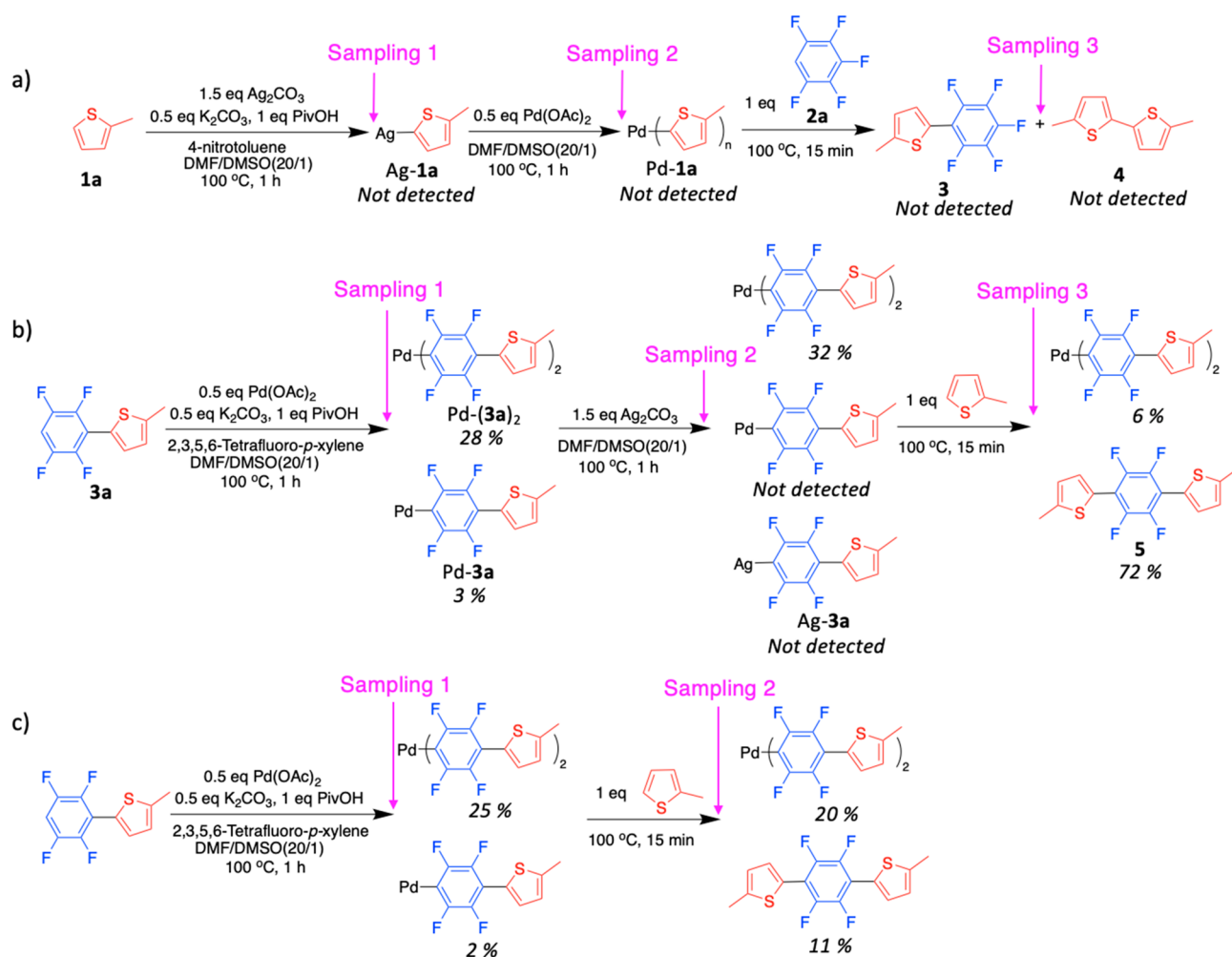
Figure 1. ^{19}F NMR spectrum of each sampling in the stepwise CDC sampling experiment shown in Scheme 4 with 2,3,5,6-tetrafluoro-*p*-xylene (-140.95 ppm in $\text{DMSO}-d_6$) as an internal standard.

out. It is worth noting that no homocoupled thiophene dimer **4** was present in any sampling in Scheme 5a, which will be explained later. When the sequence of adding Ag_2CO_3 and $\text{Pd}(\text{OAc})_2$ was reversed (Scheme 5b), 72% **5** was formed in sampling 3, and no **Ag-3a** was observed in any sampling according to ^{19}F NMR. The generation of **Pd-3a** and **Pd-(3a)₂** in sampling 1 indicates that **Pd-3a** and **Pd-(3a)₂** can form in the absence of the **Ag** additive. After addition of Ag_2CO_3 , the yield of **Pd-(3a)₂** increased slightly, and **Pd-3a** disappeared (sampling 2). Compared to the experiment where Ag_2CO_3 was added first, and $\text{Pd}(\text{OAc})_2$ was added second (Scheme 4), the yields of **Pd-3a** and **Pd-(3a)₂** were much lower (11% and 60% vs 3% and 28%), which suggests that the presence of **Ag** additive can promote the formation of fluoroaryl Pd intermediates by activating the C–H bonds of fluoroarenes. Therefore, based on the results in Scheme 5b, the proposed mechanistic sequence of the chain extension CDC still stands. In the sampling experiment shown in Scheme 5c, where the addition of Ag_2CO_3 was skipped, only 11% cross-coupled trimer **5** was produced in sampling 2, and the yield of **Pd-(3a)₂** decreased only a little. The results in Scheme 5b and 5c indicate that the **Ag** additive is required for the CDC to proceed mainly because the active intermediate **Pd-3a**, which is responsible for C–H bond activation of **1a**, cannot be generated from the inactive intermediate **Pd-(3a)₂** in the absence of the **Ag** additive. This was also observed in the mechanistic study of the first cross-coupling step performed by the Kanbara group.²⁶ Overall, the controlled stepwise CDC sampling experiments (Scheme 5) supported the proposed mechanistic sequence of the chain extension step (Scheme 4).

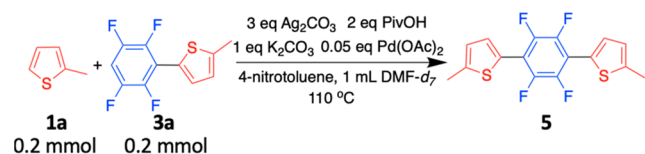
Kinetic Analysis. To obtain more information about the chain extension CDC, we performed kinetic analysis via reaction progress kinetic analysis (RPKA) and variable time normalization analysis (VTNA) based on the standard conditions shown in Scheme 6.^{27,28} The “same excess” experiment confirmed that there was no catalyst deterioration or product inhibition during the reaction (Figure 2a). The rate dependence of the important reagents was determined via VTNA. The order of zero was obtained for both **1a** and **3a**, which indicated that neither **1a** nor **3a** was involved in the rate-determining step (RDS) (Figure 2b and 2c). The first order in $[\text{Pd}]$ was determined in Figure 2d. The second order in $[\text{Ag}]$ was obtained by measuring the initial reaction rates under different AgOPiv loadings due to the poor solubility of Ag_2CO_3 in the reaction system (Figure 2e). The first order in $[\text{Pd}]$ and the second order in $[\text{Ag}]$ implied that both **Pd** and **Ag** catalysts were involved in the RDS. The second order in AgOPiv indicated that 2 equiv of AgOPiv were participating in the RDS.

The kinetic isotope effect (KIE) studies were also carried out via VTNA. As shown in Scheme 7 (note that 2 equiv of K_2CO_3 were added to reach kinetic saturation), the KIE value for the CDC between **1a** and **3a/3a-*d*₁** (Scheme 7a) was measured to be 1.1. The KIE value for the CDC between **3a** and 2-hexylthiophene/2-hexylthiophene-*d*₁ (Scheme 7b) was measured to be 1.3. The use of 2-hexylthiophene instead of **1a** was chosen because of the difficulty in synthesizing and isolating the deuterium 2-methylthiophene (**1a-*d*₁**). The results of the KIE studies verified that the RDS was not the C–H bond activation of either coupling partner.

Scheme 5. Controlled Stepwise CDC Sampling Experiments to Verify the Proposed Mechanistic Sequence of the Chain Extension Step; (a) the Sequence of Adding **1a** and **2a** Was Reversed; (b) the Sequence of Adding Ag_2CO_3 and $\text{Pd}(\text{OAc})_2$ Was Reversed; (c) the Addition of Ag_2CO_3 Was Skipped



Scheme 6. Chain Extension Step CDC under Standard Conditions for Kinetic Analysis



Origins of the High Molecular Weight/More Reactive Chain Extension CDC.

The fact that neither **1a** nor **3a** was involved in the RDS, but the Ag and Pd catalysts were both involved in RDS led us to the possibility that the oxidation of Pd(0) by Ag(I) was the RDS in the chain extension CDC. It is worth noting that in the kinetic profile of the first CDC reported by the Kanbara group,²⁶ the Pd-mediated C–H bond activation of the electron-rich thiophene species was determined to be the RDS, and that the homobifluoroaryl Pd complex ($\text{Pd}-(\text{Ar}^{\text{Pf}})_2$, [Ar^{Pf} = perfluoroarene]) was demonstrated to be a stable resting state. However, in the chain extension CDC, we found that the oxidation of Pd(0) by Ag(I) was likely the RDS. Under the same reaction conditions, the rate of oxidation is expected to remain the same in both the initial and chain extension steps. Therefore, it was surmised

that the thienyl substituent on fluorobenzene (**3a**) may have accelerated the Pd-mediated C–H bond activation on the electron-rich thiophene species in the chain extension CDC, leading to the change of RDS. This also implies that the overall rate of the chain extension CDC is faster than that of the initial step CDC. In addition, the corresponding homobifluoroaryl Pd complex ($\text{Pd}-(\mathbf{3a})_2$) may no longer be the resting state in the chain extension CDC since the concentration of fluorobenzene does not exhibit a negative rate dependence. Therefore, the chain extension CDC proceeds more efficiently than the initial step CDC, which results in high molecular weights of the D–A polymers synthesized via Pd/Ag cocatalyzed CDC. Based on our findings so far, we proposed a Pd/Ag cocatalytic cycle for the mechanism of chain extension CDC as well as the background homocoupling cycle of thiophene species (Scheme 8). The mechanism of the homocoupling side reaction of thiophene species was putatively proposed based on previous reports, where the Ag additive was determined to be the C–H bond activation reagent.^{26,29,30}

Origins of the Minimal Homocoupling Defects/High Cross Chemoselectivity. To understand of the origins of the extraordinary cross chemoselectivity in the chain extension CDC, we conducted two additional stepwise CDC sampling experiments (Scheme 9). We mixed Ag_2CO_3 , **3a** or **2a**, 2-(2-

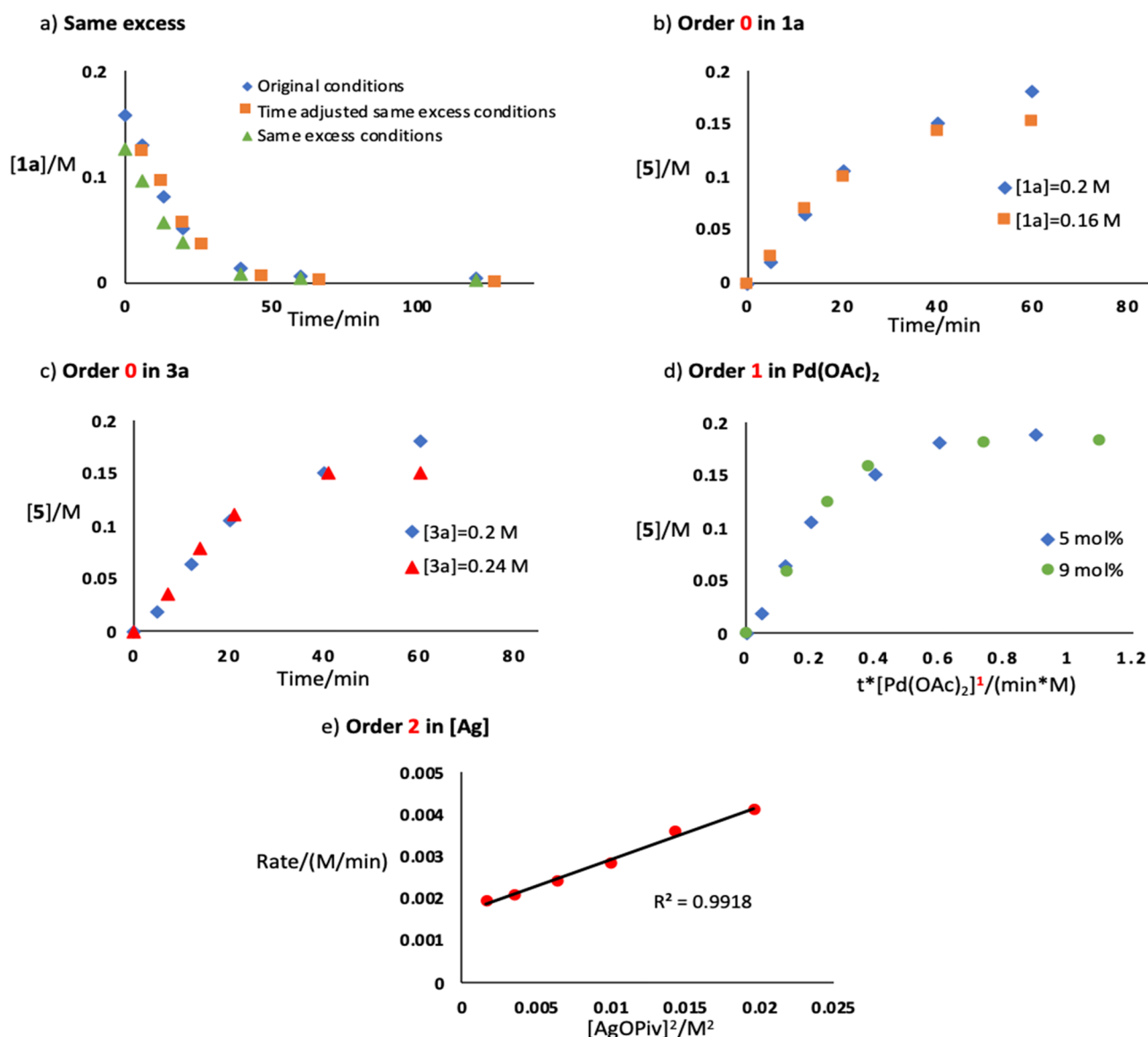
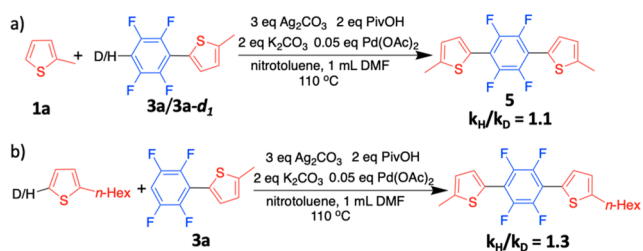


Figure 2. (a) Same excess experiment and determination of the order in (b) **1a**, (c) **3a**, (d) $\text{Pd}(\text{OAc})_2$, and (e) $[\text{Ag}]$ (due to the poor solubility of Ag_2CO_3 in DMF, a soluble Ag salt, AgOPiv , was used to determine the order in $[\text{Ag}]$).

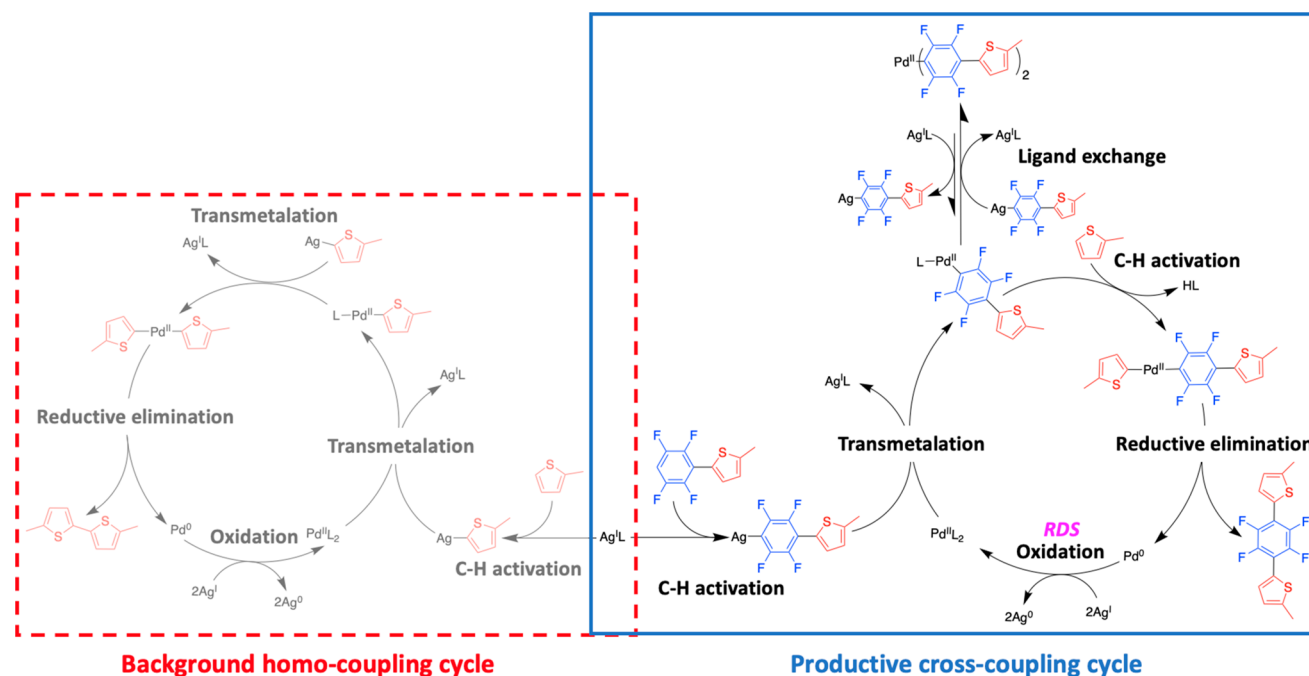
Scheme 7. KIE Studies: (a) the Reaction between **1a and **3a/3a-*d*₁** and (b) the Reaction between **3a** and 2-Hexylthiophene/2-Hexylthiophene-*d*₁**



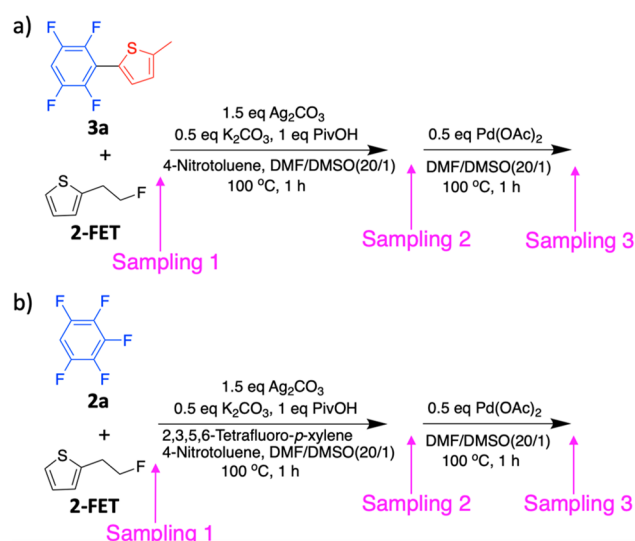
fluoroethyl)thiophene (**2-FET**), and other additives together at the beginning of the sampling experiments and tracked the yield of each species using ^1H NMR in $\text{DMSO-}d_6$ (^1H NMR spectra are shown in **Figures S11** and **S12** in the Supporting Information). We chose to use 2-(2-fluoroethyl)thiophene (**2-FET**) over 2-methylthiophene here to allow for reaction monitoring using ^{19}F NMR spectroscopy. The yields of all the

species in each sampling are summarized in **Tables 2** and **3**. Examination of sampling 2 in **Tables 2** and **3** revealed that only the fluoroaryl Ag intermediates (**Ag-2a** and **Ag-3a**) were observed. This observation was unexpected because according to our deuterium studies shown in **Tables S1** and **S2** and **Schemes S1a** and **S1c** in the Supporting Information, Ag_2CO_3 was able to cleave the C–H bonds of both thiophene and fluorobenzene arenes. Therefore, we speculated that the absence of **Ag-2-FET** is related to the relative thermodynamic stability of aryl Ag intermediates.³⁰ The fact that the yield of **2-FET** was still $\sim 100\%$ in sampling 2 in both **Tables 2** and **3** suggests that, during the 1 h between sampling 1 and sampling 2, **Ag-2-FET** was formed after C–H bond activation, but it immediately reacted with a proton source in the reaction mixture (most likely **PivOH**) to regenerate **2-FET**. After the addition of $\text{Pd}(\text{OAc})_2$ (sampling 3 in **Tables 2** and **3**), only cross-coupled products, some leftover fluoroarenes (**2a** and **3a**), and homobifluoroaryl Pd complexes ($\text{Pd}(\text{3a})_2$ and $\text{Pd}(\text{2a})_2$) were detected. No homocoupled **2-FET** dimerization product in any of the samplings in **Tables 2** and **3** implied that

Scheme 8. Proposed Mechanisms of Pd/Ag Cocatalyzed Chain Extension Step CDC as well as the Background Homo-coupling of Thiophene Species



Scheme 9. Stepwise CDC Sampling Experiments for the Mixture of 2-FET and (a) 3a or (b) 2a as the Starting Material



the formation of the homocoupled thiophene dimer requires the initial Ag-mediated C–H bond activation of the thiophene

species, followed by immediate transmetalation with a Pd(II) catalyst to generate the thienyl Pd intermediate. This supported the homocoupling catalytic cycle proposed in Scheme 8. The above observations and discussion also explained the absence of homocoupled product in Scheme 5a. The absence of Pd-2-FET in sampling 3 in both Tables 2 and 3 was probably the consequence of the instability of the thienyl Pd intermediate under the reaction conditions because Pd(II) was known to be capable of activating the C–H bonds of thiophene species.^{29,31,32} The absence of 2-FET in sampling 3 in Tables 2 and 3 suggests that the disappearance of Pd-2-FET did not regenerate the 2-FET and that deterioration was likely to happen to Pd-2-FET.

Based on the kinetic profiles of both the initial and chain extension CDCs and the discoveries about the homocoupling mechanism, the reasons for the extremely high cross chemoselectivity in the chain extension CDC as well as the nearly unnoticeable chemoselectivity in the initial step CDC can be deduced. At the beginning of either the initial or the chain extension CDC reaction, both thienyl Ag and fluoroaryl Ag intermediates can be formed via Ag-mediated C–H bond activation. In the chain extension CDC, the thienyl substituent of 3a accelerates the rate of the whole cross-coupling cycle, which makes the cross-coupling cycle much more efficient than the background dimerization of 1a. Consequently, the

Table 2. Yield of Each Species in the Stepwise CDC Sampling Experiment Shown in Scheme 9a

Sampling	3a (%)	2-FET (%)	Ag-2-FET (%)	Ag-3a (%)	Pd-2-FET (%)	Pd-3a (%)	Pd-(3a) ₂ ^a (%)	Cross-coupled product (3a-2-FET) (%)	2-FET dimerization product (%)
1	100	100	Not detected	Not detected	–	–	–	Not detected	Not detected
2	91	100	Not detected	9	–	–	–	Not detected	Not detected
3	19	Not detected	Not detected	Not detected	Not detected	Not detected	12	48	Not detected

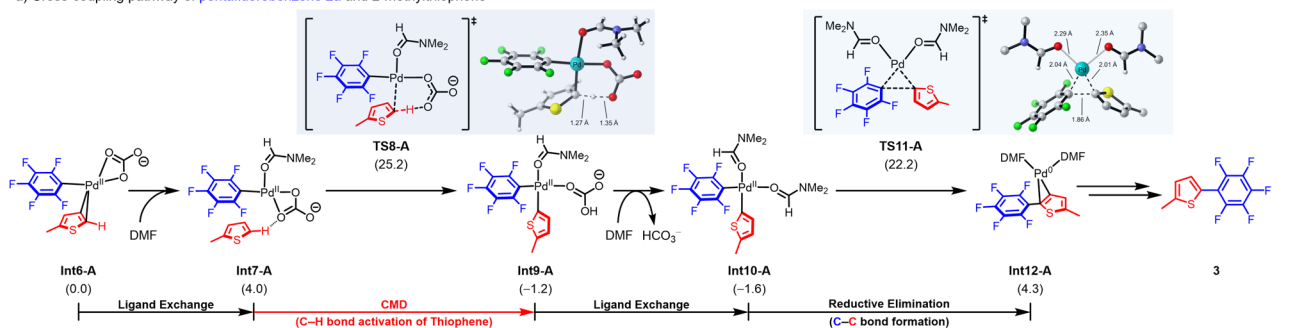
^aThe yield was obtained via ¹⁹F NMR using the same NMR sample.

Table 3. Yield of Each Species in the Stepwise CDC Sampling Experiment Shown in Scheme 9b

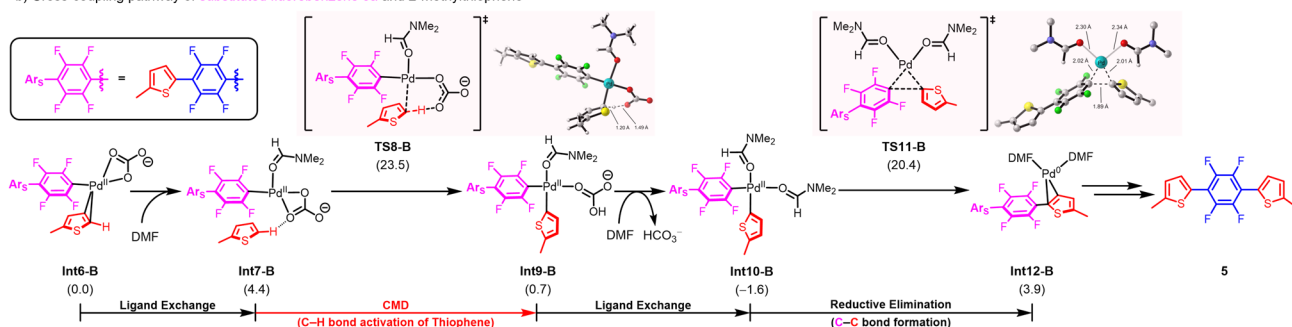
Sampling	2a ^a (%)	2-FET (%)	Ag-2-FET (%)	Ag-2a ^a (%)	Pd-2-FET (%)	Pd-2a ^a (%)	Pd-(2a) ₂ ^a (%)	Cross-coupled product (2a-2-FET) (%)	2-FET dimerization product (%)
1	100	100	Not detected	Not detected	–	–	–	Not detected	Not detected
2	69	98	Not detected	30	–	–	–	Not detected	Not detected
3	26	Not detected	Not detected	Not detected	Not detected	Not detected	38	25	Not detected

^aThe yield was obtained via ¹⁹F NMR using the same NMR sample.

a) Cross-coupling pathway of pentafluorobenzene 2a and 2-methylthiophene



b) Cross-coupling pathway of substituted fluorobenzene 3a and 2-methylthiophene



c) TS bond energy analysis of C-H bond activation

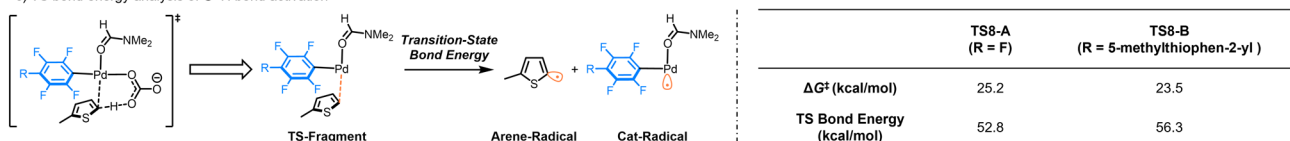


Figure 3. Computational studies of the substituent effect on the Pd-catalyzed C–H bond activation of thiophene.

fluoroaryl Ag intermediate (Ag-3a) outcompetes the thienyl Ag intermediate (Ag-1a) in the subsequent transmetalation with the Pd catalyst (only 5 mol % in the reaction). The remaining unreacted Ag-1a will react with the proton source PivOH in the reaction to regenerate 1a. This is in contrast to the initial CDC where the cross-coupling cycle with 2a progresses relatively slowly. This gives the Pd catalyst enough time to undergo transmetalation with Ag-1a and the homocoupling cycle before Ag-1a is consumed by the proton source PivOH in the reaction. The extraordinary cross chemoselectivity in the chain extension CDC leads to minimal content of homocoupling defects in the D–A polymer product.

Density Functional Theory (DFT) Calculations. To further understand the origins of the substituent effect of the thienyl group of 3a on the Pd-mediated C–H bond activation, we next explored the free energy changes using density functional theory (DFT) calculations. Figure 3a shows the DFT-computed free energy changes of the sequential C–H bond activation and reductive elimination in the cross-coupling reaction with pentafluorobenzene 2a. From the intermediate

Int6-A, DMF first coordinates to generate the intermediate Int7-A, which allows the C–H bond activation of thiophene via TS8-A. This overall C–H bond activation requires a barrier of 25.2 kcal/mol as compared to Int6-A. Subsequently, a secondary DMF exchanges the coordination of HCO₃[−], leading to the biaryl Pd(II) intermediate Int10-A. This intermediate undergoes the aryl–aryl reductive elimination via TS11-A to produce the cross-coupling product-coordinated complex Int12-A. From Int12-A, the product liberation and oxidation of Pd(0) can occur to release the observed cross-coupled dimer product 3 and regenerate the active Pd(II) catalyst. Figure 3b shows the DFT-computed free energy changes of the same processes with the cross-coupled dimer coupling partner 3a. Comparison with Int6-A revealed Int6-B has an extra thienyl substituent on the para-position of the fluorophenyl group. Int6-B undergoes the DMF exchange and subsequent C–H bond activation of thiophene via TS8-B to generate the biaryl Pd(II) intermediate Int9-B. This C–H bond activation process requires a barrier of 23.5 kcal/mol as compared to Int6-B. Subsequent aryl–aryl reductive elimi-

nation through **TS11-B** leads to the product-coordinated complex **Int12-B**, which further liberates the cross-coupled trimer product **5**.

Our computational results corroborated the above mechanistic proposal that the additional thienyl substituent in the CDC extension steps accelerates the Pd-mediated C–H bond activation and promotes the chain growth of the polymerization. Without the thienyl substituent, the C–H bond activation via **TS8-A** requires a barrier of 25.2 kcal/mol as compared to the thiophene-coordinated intermediate **Int6-A**. With the additional thienyl substituent, the Pd-mediated C–H bond activation in the CDC extension steps now requires a barrier of 23.5 kcal/mol (**Int6-B** to **TS8-B**), which corresponds to about 1 order of magnitude rate acceleration. We also verified this barrier change with calculations using additional functionals (Table S6 in Supporting Information). We believe that the additional thienyl substituent promotes the Pd–thiophene interaction in the C–H bond activation transition state **TS8-B**, which leads to the rate acceleration. This rationale is supported by the TS bond energy analysis of **TS8-A** and **TS8-B** (Figure 3c). TS bond energy analysis, developed by Ess and co-workers,³³ calculates the bond energy between the thiophene and Pd complex fragments in the C–H bond activation transition state, which provides a straightforward analysis of the strength of interaction in the transition state and has been successfully applied in the analysis of other C–H bond activation transition states. In **TS8-A**, the TS bond energy of the Pd–thiophene bond is 52.8 kcal/mol, while the same bond in **TS8-B** has a 56.3 kcal/mol interaction energy (Figure 3c). Therefore, the additional thienyl substituent in the CDC extension process strengthens the Pd–thiophene interaction in the transition state of C–H bond activation of 2-methylthiophene (**1a**). This rate acceleration of the C–H bond activation makes the chain growth faster than the initial step of the polymerization and suppresses the homocoupling side reactions, eventually resulting in the excellent polymerization performance.

CONCLUSIONS

In summary, this study shows that the Pd/Ag cocatalyzed CDC system exceeds the expectations of the Carothers equation because the reactivity of C–H bond is enhanced in the cross-coupled dimer due to the presence of the thienyl substituent. The stepwise CDC sampling experiments revealed a Pd/Ag cocatalytic cycle of the chain extension CDC, where Ag catalyst activates the C–H bond of the electron-poor fluoroaryl species, Pd catalyst activates the C–H bond of the electron-rich thiophene species, and homobifluoroaryl Pd complex is formed during the reaction as an inactive intermediate. This sequence is the same as the reaction pathway of the first CDC which was uncovered by the Kanbara group.²⁶ However, delving into the kinetics of the Pd/Ag cocatalyzed CDC system, we discovered the accelerated Pd-mediated C–H bond activation during the second cross-coupling, which results in the faster chain extension CDC than the initial CDC. This explains the high molecular weight of the produced D–A polymer. It was also demonstrated that the homocoupling pathway requires the initial Ag-mediated C–H bond activation of thiophene species, followed by immediate transmetalation with Pd catalyst. From all the findings above, it is deduced that the high cross chemoselectivity in the chain extension CDC, which leads to a perfectly alternating D–A polymer, is caused by the cross-coupling cycle in the chain

extension CDC being more efficient than the thiophene homocoupling cycle, so that in the chain extension step the cross-coupling cycle outcompetes the homocoupling cycle. Finally, free energy changes calculated by DFT revealed that the accelerated Pd-mediated C–H bond activation in the chain extension CDC is a result of the lowered energy barrier required for the Pd-mediated C–H bond activation (25.2 without the thienyl substituent, 23.5 kcal/mol with the thienyl substituent). The lowered energy barrier is attributed to the stronger Pd–thiophene interaction in the C–H bond activation transition state in the presence of an additional thienyl substituent on the fluoroaryl coupling partner. The work provides valuable insight for future studies in obtaining high-molecular weight D–A semiconducting polymers. More broadly speaking, this work has implications in small molecule synthesis—introduction of the thiophene has a significant effect on the chemoselectivity in the CDC reaction offering a method to engineer the substrate structure to enhance the utility of C–H activation.

ASSOCIATED CONTENT

Supporting Information

The Supporting Information is available free of charge at <https://pubs.acs.org/doi/10.1021/jacs.1c12599>.

General methods and materials; deuterium studies of CDC; results of the controlled stepwise CDC sampling experiments; NMR spectra of stepwise CDC sampling experiments; general methods of kinetic analysis; kinetic isotope effect studies; synthesis of deuterated substrates; and verification of rate acceleration by various functionals (PDF)

AUTHOR INFORMATION

Corresponding Authors

Christine K. Luscombe – Molecular Engineering & Sciences Institute, University of Washington, Seattle, Washington 98195, United States; Material Science & Engineering Department and Department of Chemistry, University of Washington, Seattle, Washington 98195, United States; Present Address: pi-Conjugated Polymers Unit, Okinawa Institute of Science and Technology Graduate University, Okinawa, Japan, 904–0495; orcid.org/0000-0001-7456-1343; Email: christine.luscombe@oist.jp

Kendall N. Houk – Department of Chemical and Biomolecular Engineering and Department of Chemistry and Biochemistry, University of California Los Angeles, Los Angeles, California 90095, United States; orcid.org/0000-0002-8387-5261; Email: hok@chem.ucla.edu

Xin Hong – Center of Chemistry for Frontier Technologies, Department of Chemistry, State Key Laboratory of Clean Energy Utilization, Zhejiang University, Hangzhou 310027, China; Key Laboratory of Precise Synthesis of Functional Molecules of Zhejiang Province, School of Science, Westlake University, Hangzhou 310024 Zhejiang Province, China; orcid.org/0000-0003-4717-2814; Email: hxchem@zju.edu.cn

Authors

Liwen Xing – Molecular Engineering & Sciences Institute, University of Washington, Seattle, Washington 98195, United States

Ji-Ren Liu – Center of Chemistry for Frontier Technologies, Department of Chemistry, State Key Laboratory of Clean Energy Utilization, Zhejiang University, Hangzhou 310027, China; Key Laboratory of Precise Synthesis of Functional Molecules of Zhejiang Province, School of Science, Westlake University, Hangzhou 310024 Zhejiang Province, China

Complete contact information is available at:

<https://pubs.acs.org/10.1021/jacs.1c12599>

Author Contributions

[†]L.X. and J.-R. L. contributed equally.

Notes

The authors declare no competing financial interest.

ACKNOWLEDGMENTS

This work was supported by the NSF under the CCI Center for Selective CH Functionalization, CHE-1700982 (partial support for L.X.) and the U.S. Department of Energy (DOE), Office of Science, Basic Energy Sciences (BES), under Award DE-SC0020046 (reagent purchase). National Natural Science Foundation of China (21702182, 21873081, and 22122109, X.H.), the Fundamental Research Funds for the Central Universities (2020XZZX002-02, X.H.), the State Key Laboratory of Clean Energy Utilization (ZJUCEU2020007, X.H.), the Starry Night Science Fund of Zhejiang University Shanghai Institute for Advanced Study (SN-ZJU-SIAS-006, X.H.), and the Center of Chemistry for Frontier Technologies and Key Laboratory of Precise Synthesis of Functional Molecules of Zhejiang Province (PSFM2021-01, X.H.) are gratefully acknowledged. Calculations were performed on the high-performance computing system at Department of Chemistry, Zhejiang University.

REFERENCES

- (1) Carothers, W. H. Polymers and Polyfunctionality. *Trans. Faraday Soc.* **1936**, *32*, 39.
- (2) Odian, G. *Principles of Polymerization*, 4th ed.; Wiley: New York, 2004.
- (3) Iimori, H.; Shibasaki, Y.; Ando, S.; Ueda, M. Nonstoichiometric Polycondensation I. Synthesis of Polythioether from Dibromomethane and 4,4'-Thiobisbenzenethiol. *Macromol. Symp.* **2003**, *199*, 23–36.
- (4) Matyjaszewski, K.; Möller, M. *Polymer Science: A Comprehensive Reference*, Vol. 5; Elsevier: Amsterdam, 2013.
- (5) Miyatake, K.; Hlil, A. R.; Hay, A. S. High Molecular Weight Aromatic Polyformals Free of Macrocyclic Oligomers. A Condensative Chain Polymerization Reaction. *Macromolecules* **2001**, *34*, 4288–4290.
- (6) Kihara, N.; Komatsu, S.; Takata, T.; Endo, T. Significance of Stoichiometric Imbalance in Step Polymerization via Reactive Intermediate. *Macromolecules* **1999**, *32*, 4776–4783.
- (7) Goto, E.; Ando, S.; Ueda, M.; Higashihara, T. Nonstoichiometric Stille Coupling Polycondensation for Synthesizing Naphthalene-Diimide-Based π -Conjugated Polymers. *ACS Macro Lett.* **2015**, *4*, 1004–1007.
- (8) Kang, L. J.; Xing, L.; Luscombe, C. K. Exploration and Development of Gold- and Silver-Catalyzed Cross Dehydrogenative Coupling toward Donor–Acceptor π -Conjugated Polymer Synthesis. *Polym. Chem.* **2019**, *10*, 486–493.
- (9) Nambiar, S.; Yeow, J. T. W. Conductive Polymer-Based Sensors for Biomedical Applications. *Biosens. Bioelectron.* **2011**, *26*, 1825–1832.
- (10) Siringhaus, H. 25th Anniversary Article: Organic Field-Effect Transistors: The Path Beyond Amorphous Silicon. *Adv. Mater.* **2014**, *26*, 1319–1335.

(11) Holliday, S.; Li, Y.; Luscombe, C. K. Recent Advances in High Performance Donor-Acceptor Polymers for Organic Photovoltaics. *Prog. Polym. Sci.* **2017**, *70*, 34–51.

(12) Liu, C.; Wang, K.; Gong, X.; Heeger, A. J. Low Bandgap Semiconducting Polymers for Polymeric Photovoltaics. *Chem. Soc. Rev.* **2016**, *45*, 4825–4846.

(13) Miyaura, N.; Yamada, K.; Suzuki, A. A New Stereospecific Cross-Coupling by the Palladium-Catalyzed Reaction of 1-Alkenylboranes with 1-Alkenyl or 1-Alkynyl Halides. *Tetrahedron Lett.* **1979**, *20*, 3437–3440.

(14) Stille, J. K. The Palladium-Catalyzed Cross-Coupling Reactions of Organotin Reagents with Organic Electrophiles [New Synthetic Methods(58)]. *Angew. Chem., Int. Ed. Engl.* **1986**, *25*, 508–524.

(15) Bura, T.; Blaskovits, J. T.; Leclerc, M. Direct (Hetero)Arylation Polymerization: Trends and Perspectives. *J. Am. Chem. Soc.* **2016**, *138*, 10056–10071.

(16) Osedach, T. P.; Andrew, T. L.; Bulović, V. Effect of Synthetic Accessibility on the Commercial Viability of Organic Photovoltaics. *Energy Environ. Sci.* **2013**, *6*, 711.

(17) Vangerven, T.; Verstappen, P.; Drijkoningen, J.; Dierckx, W.; Himmelberger, S.; Salleo, A.; Vanderzande, D.; Maes, W.; Manca, J. v. Molar Mass versus Polymer Solar Cell Performance: Highlighting the Role of Homocouplings. *Chem. Mater.* **2015**, *27*, 3726–3732.

(18) Hendriks, K. H.; Li, W.; Heintges, G. H. L.; van Pruijsen, G. W. P.; Wienk, M. M.; Janssen, R. A. J. Homocoupling Defects in Diketopyrrolopyrrole-Based Copolymers and Their Effect on Photovoltaic Performance. *J. Am. Chem. Soc.* **2014**, *136*, 11128–11133.

(19) Stuart, D. R.; Fagnou, K. The Catalytic Cross-Coupling of Unactivated Arenes. *Science* **2007**, *316*, 1172–1175.

(20) Aoki, H.; Saito, H.; Shimoyama, Y.; Kuwabara, J.; Yasuda, T.; Kanbara, T. Synthesis of Conjugated Polymers Containing Octafluorobiphenylene Unit via Pd-Catalyzed Cross-Dehydrogenative-Coupling Reaction. *ACS Macro Lett.* **2018**, *7*, 90–94.

(21) Zhang, Q.; Chang, M.; Lu, Y.; Sun, Y.; Li, C.; Yang, X.; Zhang, M.; Chen, Y. A Direct C–H Coupling Method for Preparing π -Conjugated Functional Polymers with High Regioregularity. *Macromolecules* **2018**, *51*, 379–388.

(22) Xing, L.; Luscombe, C. K. Advances in Applying C–H Functionalization and Naturally Sourced Building Blocks in Organic Semiconductor Synthesis. *J. Mater. Chem. C* **2021**, *9*, 16391–16409.

(23) Cambeiro, X. C.; Ahlsten, N.; Larrosa, I. Au-Catalyzed Cross-Coupling of Arenes via Double C–H Activation. *J. Am. Chem. Soc.* **2015**, *137*, 15636–15639.

(24) Liu, J.-R.; Duan, Y.-Q.; Zhang, S.-Q.; Zhu, L.-J.; Jiang, Y.-Y.; Bi, S.; Hong, X. C–H Acidity and Arene Nucleophilicity as Orthogonal Control of Chemoselectivity in Dual C–H Bond Activation. *Org. Lett.* **2019**, *21*, 2360–2364.

(25) Blaskovits, J. T.; Johnson, P. A.; Leclerc, M. Mechanistic Origin of β -Defect Formation in Thiophene-Based Polymers Prepared by Direct (Hetero)Arylation. *Macromolecules* **2018**, *51*, 8100–8113.

(26) Shimoyama, Y.; Kuwabara, J.; Kanbara, T. Mechanistic Study of Pd/Ag Dual-Catalyzed Cross-Dehydrogenative Coupling of Perfluoroarenes with Thiophenes. *ACS Catal.* **2020**, *10*, 3390–3397.

(27) Blackmond, D. G. Reaction Progress Kinetic Analysis: A Powerful Methodology for Mechanistic Studies of Complex Catalytic Reactions. *Angew. Chem., Int. Ed.* **2005**, *44*, 4302–4320.

(28) Burés, J. Variable Time Normalization Analysis: General Graphical Elucidation of Reaction Orders from Concentration Profiles. *Angew. Chem., Int. Ed.* **2016**, *55*, 16084–16087.

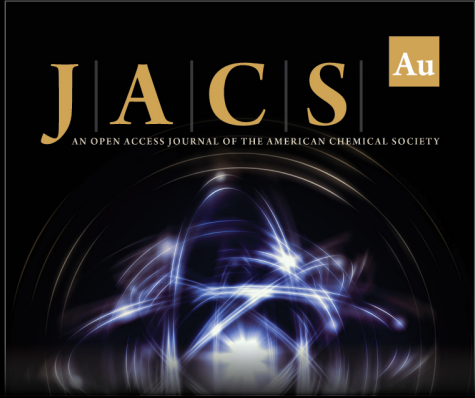
(29) Masui, K.; Ikegami, H.; Mori, A. Palladium-Catalyzed C–H Homocoupling of Thiophenes: Facile Construction of Bithiophene Structure. *J. Am. Chem. Soc.* **2004**, *126*, 5074–5075.

(30) Lotz, M. D.; Camasso, N. M.; Cauty, A. J.; Sanford, M. S. Role of Silver Salts in Palladium-Catalyzed Arene and Heteroarene C–H Functionalization Reactions. *Organometallics* **2017**, *36*, 165–171.


(31) Fujinami, Y.; Kuwabara, J.; Lu, W.; Hayashi, H.; Kanbara, T. Synthesis of Thiophene- and Bithiophene-Based Alternating Copolymers via Pd-Catalyzed Direct C–H Arylation. *ACS Macro Lett.* **2012**, *1*, 67–70.

(32) Wang, L.; Carrow, B. P. Oligothiophene Synthesis by a General C–H Activation Mechanism: *Electrophilic* Concerted Metalation–Deprotonation (*e* CMD). *ACS Catal.* **2019**, *9*, 6821–6836.


(33) Petit, A.; Flygare, J.; Miller, A. T.; Winkel, G.; Ess, D. H. Transition-State Metal Aryl Bond Stability Determines Regioselectivity in Palladium Acetate Mediated C–H Bond Activation of Heteroarenes. *Org. Lett.* **2012**, *14*, 3680–3683. Details on calculations for TS bond energy are included in [Supporting Information](#).




JACS Au
AN OPEN ACCESS JOURNAL OF THE AMERICAN CHEMICAL SOCIETY



Editor-in-Chief
Prof. Christopher W. Jones
Georgia Institute of Technology, USA

Open for Submissions 

pubs.acs.org/jacsau  ACS Publications
Most Trusted. Most Cited. Most Read.